



Properties of Acrylonitrile-Butadiene-Styrene nanocomposites adding ammonia plasma treated carbon nanotubes/graphene nanoplatelets for electronic discharge application

Sorawit DUANGSRIPAT¹, Pajaera PATANATHABUTR¹, and Nattakarn HONGSRIPHAN^{1,*}

¹ Department of Materials Science and Engineering, Faculty of Engineering and Industrial Technology, Silpakorn University, Nakhon Pathom 73000, Thailand

*Corresponding author e-mail: Hongsriphan_N@silpakorn.edu

Received date:
25 March 2024

Revised date:
7 May 2024

Accepted date:
29 May 2024

Keywords:

Graphene nanoplatelet (GNP);
Carbon nanotube (CNT);
Plasma functionalization;
Acrylonitrile-Butadiene-
Styrene (ABS);
Electronic packaging material

Abstract

Carbon-based nanofillers have been applied in various products, especially electrical and electronic products. It could be used to modify electrical conductivity of the integrated circuit (IC) polymeric packaging in order to prevent electrostatic discharge that would damage electronic integrity. This research reported the influence of ammonia plasma functionalization and its concentration on electrical, mechanical and thermal properties of Acrylonitrile-Butadiene-Styrene (ABS) reinforced with a mixture of CNTs and GNPs. Nanocomposites were successfully compounded using a twin-screw extruder, which firstly the masterbatch was prepared and then mixed with neat polymer into various concentrations (2 wt%, 4 wt%, 6 wt%, and 8 wt%). It was found that ammonia plasma functionalization increased the dispersion of nanofillers in the ABS matrix. When using a hybrid nanofillers in the weight ratio of CNTs:GNPs 60:40, it was found that the percolation threshold could be reached with a nanofiller concentration of 4 wt%. The surface electrical resistivity of the NH₃-functionalized hybrid nanocomposites was reduced more than those adding the non-functionalized hybrid nanofillers. At this suitable weight ratio, tensile modulus of the CNT-NH₃:GNP-NH₃ 60:40 of 2 wt%, 4 wt%, 6 wt%, and 8 wt% could enhance the tensile modulus of ABS to be 35.98%, 38.29%, 43.54%, and 45.48% higher than that of neat ABS, respectively. Interestingly, the nanocomposites still had the ultimate tensile strength presented at yield with higher values. In addition, the NH₃-plasma functionalized nanofillers enhanced thermal conductivity of the ABS matrix much better than the non-functionalized ones, which these nanofillers could provide heat transfer by heat dissipation thoroughly in the polymer matrix.

1. Introduction

Acrylonitrile Butadiene Styrene (ABS) [1] is an amorphous engineering thermoplastics polymerized from three monomers; acrylonitrile, butadiene, and styrene, which the polymerization reaction can be done via emulsion or continuous mass process. The natural color of ABS is opaque ivory. Commercially grade ABS could have various impact resistance depending on the monomer concentration. It provides desirable properties, such as high rigidity, resistance to impact, and good abrasion resistance, to be selected for structural applications. Neat ABS or the blends or the ABS-based composites could be fabricated for automotive parts, electronic housings, consumer products, and power tools. They are also suitable to be produced as integrated circuit (IC) tray or packaging for personal computer and electronic devices. Nonetheless, some electrical/electronic applications require polymeric material that could possess suitable conductive properties rather than just being insulating to prevent damage from electrostatic discharge (ESD). This could be achieved by adding a conductive filler into polymer matrix to obtain conductively polymeric composites. For a random distribution of any conductive filler inside the polymer matrix, a conductive network will form at a specific

loading (or concentration), which is identified as the percolation threshold [2]. When the filler loading reaches this percolation threshold, the conductivity of the polymeric composite rises suddenly which the characteristic graph between electrical conductivity and filler loading presents the S-shape, which could be summarized into three regions; insulating, percolating and conductive.

Electrostatic discharge (ESD) [3] is mostly created by the contact and then separation of two materials. When the two materials are in contact and then separate, electron is transferred between the two materials. One of them that losses electron results in a positive charge on the surface, and the other that gains electron becomes a negative charge on its surface. As a result, electric potentials of the two materials are different expressing as electrostatic voltage. To eliminate the electrostatic voltage, the positive charge is transferred to the negative charge. This charge transfer is known as ESD. In the other words, it is basically the sudden flow of electrical current between two objects with a different electrical charge when there is a conducting path between them.

However, if the level of electrostatic voltage is high enough, a great many charges carrying energy is rapidly transferred to the sensitive material. Thus, the sensitive material is suddenly destroyed by ESD

attack. In the electronics industry [4], ESD can be occurred on the devices throughout touch of charged human bodies to the devices, move of devices across machine surfaces, slide of devices in packages, or induction of electrostatic fields, etc. Occurred ESD can easily damage the sensitive devices in the form of an arc or spark at the sufficiently difference potentials. Accordingly, the sensitive device fails immediately or loss their electrical characteristics. Furthermore, reduction of device sizes to increase speed and decrease power consumption today cause increment of their sensitivity to ESD damage at very low electrostatic voltages. Consequently, static safe techniques such as grounding, ionization, and the use of conductive packaging materials have been developed to products from ESD.

One of the static safe techniques that can directly protect the devices from ESD charges is the use of conductive packaging materials [5-7]. When surface of the conductive packaging becomes charged by rubbing between the device and the packaging, the charges are allowed to dissipate across its surface or through its volume and then transfer to ground or another nearby conductive object in order to reduce the electrostatic voltage to the low level. As a result, ESD event is not violent enough to damage the device. Accordingly, the conductive packaging materials can safely protect the devices from ESD event by limiting the passage of ESD current and reducing the energy that causes from ESD. Moreover, they can shield the electrostatic fields which induce charges to accumulate on the devices and create ESD. Typically, the material's ability to prevent ESD damage is measured by surface electrical resistivity [8]. Conductive compounds which have surface electrical resistivity values in a range of $10^3 \Omega \cdot \text{sq}^{-1}$ to $10^9 \Omega \cdot \text{sq}^{-1}$ can be used to directly protect from ESD event.

Electronic packaging materials [9] are most commonly made from conductive compounds which are melt compounded from thermoplastic pellets and conductive fillers. The common conductive fillers or antistatic agents are carbon black (CB) [5,7], carbon nanotube (CNTs) [8] and expanded graphite [10]. Unfortunately, compounding these carbon-based fillers into polymer matrix turn the color of the composites to be super black that might limit them to be used in electrical/electronic applications. Moreover, adding too high concentrations of these fillers cause them to be aggregated inside the polymer matrix and the composites are more rigid with brittle behaviour. CB is widely used in the industries since it is inexpensive, however, it has to be used in high concentration for electrical conductivity and causes toughness reduction. The nanosized CNTs can significantly increase electrical conductivity of polymer composites at low concentration (0.1 vol%) [11], but the it is considered an expensive filler.

Al-Saleh [8] blended hydrophobic polypropylene with organoclay/CNTs in various concentrations, which they discussed a percolation threshold model of the nanocomposites that it was typically presented in three major zones. In the first zone, the concentration of conductive nanofillers was still too low, they were apart from each other resulting the electrical conductivity was similar to that of neat polymer. For polypropylene adding CNTs and organoclay composites (PP/CNT:OMC), this zone extended from 0 wt% CNTs to CNTs of 0.25 wt%. In the second zone, the concentration of conductive nanofiller particles reached a critical concentration at which the electrical conductivity increased suddenly in a significant value. It indicated the formation of the first 3D conductive network within the polymer matrix, at which

this zone occurred at around CNTs of 0.5 wt% in the PP/CNT:OMC composite. Finally, the third zone occurred at the filler concentrations above the electrical percolation, which was characterized by an increase in electrical conductivity with the nanofiller concentration. This implied the increase in the number of conductive pathways within the nanocomposite.

Compared with CNTs, the price of graphene nanoplatelets (GNPs) is lower and there is plenty of pristine graphite for starting its plasma synthesis, it is thus considered to be an ideal choice to be applied as a conductive filler in the preparation of conductive polymer-based nanocomposites. Basically, a percolation threshold could be reached with lower GNP concentration than that by graphite. According to Caradonna *et al.* [12], percolation thresholds for CNTs, GNPs, and graphite occurred at 1.34×10^{-1} vol% (0.2 wt%), 9.21 vol% (15 wt%), and 21.96 vol% (35 wt%), respectively. They discussed that the alignment of CNTs in the direction along with the electrical conductivity measured was the key of electrical conductivity enhancement.

Yang *et al.* [13] reported that the high aspect ratio and the large specific surface area of GNPs led to a high contact area between composites and nanofillers and caused a maximized transferred stress and phonon transference from the matrix to the nanofillers. Therefore, the GNP-reinforced composites can be expected to exhibit better electrical, mechanical, and thermal properties even in comparison to CNTs. In addition, thermal conductivity of the epoxy composites adding GNPs [14] was studied and found that the composites achieved a significant increase in in-plane thermal conductivity with GNPs of 2.0 wt%, and it could be applied for electronic packaging material.

An interesting treatment for adding functional groups to CNTs or GNPs which could improve physical compatibility and better dispersion with polymeric matrix is by plasma treatment [15,16]. Williams *et al.* [16] reported effect of plasma treatment on CNTs in the presence of oxygen and ammonia, which they proposed that the treatment could be scaled up for relatively large quantities. The plasma treatment changed the surface chemistry as well as the morphology of the CNTs. There was an increase in oxygen species for the oxygen-treated CNTs, such as carbonyl, hydroxyl, and carboxyl being grafted to the surface. For the ammonia treatment, there was nitrogen species corresponding to amine, nitrile, amide, and oxime groups onto the surface of the CNTs. Then, the plasma-treated CNTs were mixed in epoxy resin, which the improvement in dispersion was achieved.

This research work was aimed to determine the suitable weight ratio and the concentration of a hybrid nanofiller between CNTs and GNPs for ABS matrix in order to produce an electronic packaging material. An injection molded grade ABS were melt compounded with either CNTs, GNPs, or a hybrid nanofiller of CNTs: GNPs in 60:40 wt% and 80:20 wt%. Two types of synthesized nanofillers were applied; non-functionalized and ammonia plasma functionalized ones. The nanofiller concentration in the ABS nanocomposites was varied 2 wt%, 4 wt%, 6 wt%, and 8 wt%. The electrically conductive property of the nanocomposites was determined via surface electrical resistivity measurement. Mechanical properties of injection molded specimens were determined using tensile testing, and thermal conductivity of compression-molded nanocomposites were studied using thermal conductivity testing.

2. Materials and experimental

2.1 Materials

Acrylonitrile-Butadiene-Styrene (ABS, GA800, injection molding grade, MFI of 20 (10 kg·220°C)) was kindly provided by IRPC Public Company Limited, Thailand. Four kinds of nanofillers were used; non-functionalized carbon nanotube (CNT-R1), non-functionalized graphene (GNP-R1), ammonia plasma functionalized carbon nanotube (CNT-NH₃), and ammonia plasma functionalized graphene (GNP-NH₃). They were kindly supported by Haydale Technologies Co., Ltd., Thailand. In addition, these nanofillers were added to reinforce the ABS matrix as a hybrid nanofiller mixed in the CNTs:GNPs weight ratio of 0:100, 60:40, 80:20, and 100:0.

According to the supplier [17], the basic properties of GNPs are a bulk density of about 2.15 g·cm⁻³, a specific surface area of about ~25 m²·g⁻¹, a typical GNP planar size of 0.3 μm to 5.0 μm (SEM), and a typical GNP thickness of less than 50 nm (SEM). For CNTs, the basic properties are a bulk density of about 1.30 g·cm⁻³, a specific surface area of about 250 m²·g⁻¹ to 300 m²·g⁻¹, a typical length of ~1500 μm (SEM) and a typical outside diameter of ~9.50 nm (SEM). As presented in the supplier's data-sheet, the synthesized CNTs and GNPs were plasma functionalized by ammonia gas to obtain Amines [NH_x], Amide [RCONH₂], and Nitrous Oxide [NO_x] onto the surface of the nanofillers.

2.2 Masterbatch preparation

The ABS-based masterbatches were prepared using an internal mixer (Thermo Scientific Haake model Rheomax OS) at 200°C and a rotor speed of 60 rpm for 12 min. The nanofiller concentration was 10 phr (part per hundred of resin) in the masterbatch.

2.3 Compounding of nanocomposites

The nanocomposites were com-pounded by diluting the masterbatch with neat ABS pellets, which the final concentrations of nanofiller were 2.0 wt%, 4.0 wt%, 6.0 wt%, and 8.0 wt%. The melt compounding was performed using a twin-screw extruder (CT model CTE-D22L32, Chareon Tut Co., Ltd, Thailand) with the temperature profile of 200°C, 210°C, 220°C, 230°C, 240°C, and 240°C and a screw speed of 80 rpm. The extrudate was water cooled and then pelletized by a pelletizer. Table 1 presents abbreviations and compositions of ABS/ CNTs:GNPs nanocomposites, which the “P” letter indicates the non-functionalized (R1) or the ammonia plasma functionalized (NH₃) nanofillers.

Prior to fabrication, the ABS-based composite pellets were dried in an air-circulating oven at 70°C overnight. The composite pellets were hydraulically pressed using a hot-pressing machine (LabTech model LP-S-20, Thailand) at 210°C to prepare square-shaped specimens for surface electrical resistivity testing. For tensile testing, the dogbone-shaped specimens were injection molded using an injection molding machine (Battenfeld model BA250CDC, Austria). The injection molding temperature profile were set at 180°C, 190°C, 200°C, and 200°C. The mold temperature was 50°C.

2.4 Characterization and testing

Surface electrical resistivity measurement was measured by a surface resistance meter, Model TR1380 (Figure 1). The sheet resistance of the specimen was read in Ω·sq⁻¹, which the data come from a single measurement from one hot-pressed sheet.

The injection molded specimens were measured tensile properties in accordance to ASTM-D638 (type V) using a Tinius Olsen instrument model H50KS. The load cell was 10 kN, and the crosshead speed was set at 50 mm·min⁻¹. For each composite composition, five specimens were tested, which the averages and the standard deviations were reported.

Table 1. Abbreviations and compositions of ABS/CNTs:GNPs nanocomposites.

Abbreviations	ABS	CNTs	GNPs
Neat ABS	100.0	0.0	0.0
0CNT-P(2)	98.0	0.0	2.0
0CNT-P(4)	96.0	0.0	4.0
0CNT-P(6)	94.0	0.0	6.0
0CNT-P(8)	92.0	0.0	8.0
60CNT-P(2)	98.0	1.2	0.8
60CNT-P(4)	96.0	2.4	1.6
60CNT-P(6)	94.0	3.6	2.4
60CNT-P(8)	92.0	4.8	3.2
80CNT-P(2)	98.0	1.6	0.4
80CNT-P(4)	96.0	3.2	0.8
80CNT-P(6)	94.0	4.8	1.2
80CNT-P(8)	92.0	6.4	1.6
100CNT-P(2)	98.0	2.0	0.0
100CNT-P(4)	96.0	4.0	0.0
100CNT-P(6)	94.0	6.0	0.0
100CNT-P(8)	92.0	8.0	0.0

where P = R1 or NH₃



Figure 1. Surface electrical resistivity measurement.

Thermal conductivity of the composite sample was evaluated using a thermal constants analyzer (Model TCA TA-01). The hot-pressed specimens with a square shape (20.0 mm × 20.0 mm × 3.0 mm) were conditioned at 23°C and 50% relative humidity for 48 h. For testing, a disk sensor was placed between two pieces of the compressed samples, and then heated by a constant electrical current for a short period of time. The generated heat caused a rise in temperature of both the sensor and the sample material. The average transient temperature increased of the sensor, in an order of 0.5 K to 5.0 K, was simultaneously measured by monitoring a change in electrical resistance. Then, thermal conductivity was calculated from the temperature coefficient of resistivity of the sensor material, which correlated the change in resistivity with the corresponding change in temperature.

3. Results and Discussion

3.1 Surface electrical resistivity of ABS/carbon reinforced nanocomposites adding non-functionalized (R1) and ammonia plasma functionalized (NH₃) CNTs and GNPs

Since the goal of this research was to investigate impact of incorporating these carbon-based nanofillers into polymer material in order to protect IC packaging from ESD charges, the improvement of electrical conductivity was simply determined by means of surface electrical resistivity. Figure 2 and Figure 3 present the surface electrical resistivity of the ABS nanocomposites adding non-functionalized and ammonia plasma functionalized nanofillers, respectively. Typically, adding graphite-like filler (i.e. carbon black [7] or carbon nanotube [11]) could enhance electrical conductivity of the electrically-insulating polymer.

Neat ABS had the surface electrical resistivity of $\sim 10^{14} \Omega \cdot \text{sq}^{-1}$, which could be classified as an insulating material having the resistivity greater than $10^{12} \Omega \cdot \text{sq}^{-1}$. For 100CNT-P2 nanocomposite with the lowest CNT concentration of 2.0 wt%, the surface electrical resistivity was sharply decreased to $\sim 10^4 \Omega \cdot \text{sq}^{-1}$ to $10^5 \Omega \cdot \text{sq}^{-1}$, which was designated as a static dissipative material having the surface electrical resistivity in the range of $10^5 \Omega \cdot \text{sq}^{-1}$ to $10^9 \Omega \cdot \text{sq}^{-1}$. This implied that the percolation threshold occurred at the CNT concentration of 2.0 wt% for the ABS-based nanocomposites. Above this critical CNT concentration, the surface electrical resistivity value was reduced successively until reaching $\sim 10^1 \Omega \cdot \text{sq}^{-1}$ when CNT concentration was increased successively up to 8 wt%, which could be classified as a conductively polymeric composite.

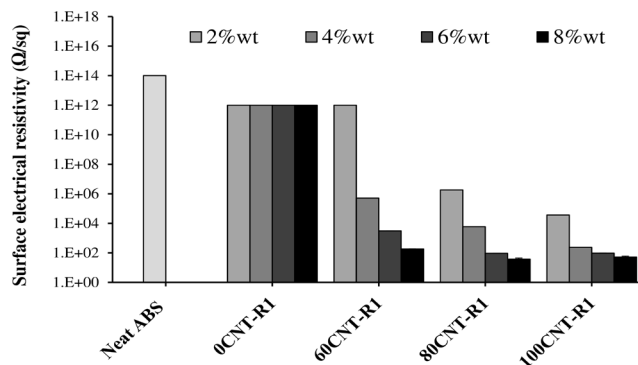


Figure 2. Surface electrical resistivity of neat ABS and ABS/non-functionalized hybrid nanocomposites.

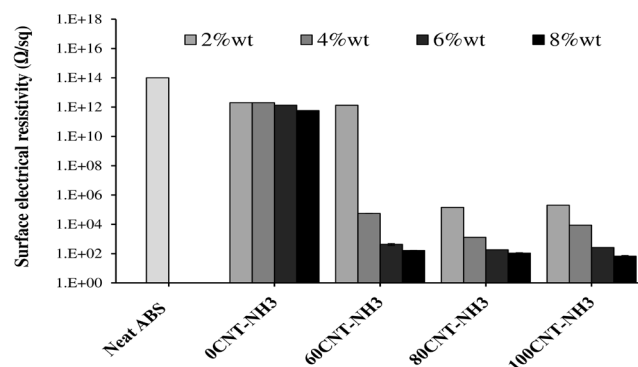


Figure 3. Surface electrical resistivity of neat ABS and ABS/ammonia plasma functionalized hybrid nanocomposites.

The decrease in surface electrical resistivity of the nanocomposites with an addition of either CNT-R1 (Figure 2) or CNT-NH₃ (Figure 3) above 2 wt% could be explained by the percolation theory [2]. The percolation threshold [11] is defined as the minimum concentration of conductive filler in the insulating matrix which is characterized by a sharp increase in electrical conductivity due to the formation of conductive network and realize an insulator-to-conductor transition in the composites. Dul *et al.* [18] reported the similar results when they compounded non-functionalized CNT into ABS matrix and found that the percolation threshold was 2.0 wt%.

It is well known that the electrical conduction through the bulk of any compound is controlled by a number of paths (or the aggregate chains). As the number of particles increased, the number of continuous chain or conductive path through the compound increases. The total electrical resistance for any chain consists of the sum of individual electrical resistance at each point of contact. For this research, this was attributed to the very much higher fiber aspect ratio of the CNTs than that of the GNPs. For CNTs, the supplier reports that a typical length of $\sim 1500 \mu\text{m}$ with a typical outside diameter of $\sim 9.5 \text{ nm}$. This could be attributed to these filament-like nanofillers are distributed inside the ABS matrix to form network nodes for electrical conductivity.

On the other hand, the 0CNT nano-composites adding either GNP-R1 or GNP-NH₃ in the concentration range of 2.0 wt% to 8.0 wt%, the surface electrical resistivity value of $\sim 10^{12} \Omega \cdot \text{sq}^{-1}$ to $10^{11} \Omega \cdot \text{sq}^{-1}$ was still in the electrical insulating range. This implied an insufficient concentration of GNPs to create the percolation threshold. Dul *et al.* [18] reported the similar results when they compounded non-functionalized

GNPs into ABS matrix and found that the percolation threshold was higher than 8 wt%.

For GNPs, the supplier reports that the GNPs have a typical GNP planar size of 0.3 μm to 5.0 μm and a typical GNP thickness of less than 50 nm. According to Du *et al.* [19], the percolation threshold of the HDPE composites adding CNTs was lower than those adding GNPs. This resulted from the aggregation and the wrinkle of GNPs that lowered their effective aspect ratios and the network formation was hindered.

When using a hybrid nanofillers (mixing GNPs with less expensive CNTs) in the weight ratio of 60:40 wt%, it was found that the percolation threshold could be reached with a nanofiller concentration of 4 wt%, at which the surface electrical resistivity of the NH_3 -hybrid nanocomposites was reduced more than those adding the R1-hybrid nanofillers.

Claypole *et al.* [20] studied rheological properties of the non-functionalized and NH_3 -plasma functionalized GNPs, which were also supplied by Haydale Technologies. They reported that the NH_3 plasma functionalization prevented the treated nanofillers to be agglomerated. Thus, these nanofillers were dispersed in nanoscale size having a high aspect ratio. When they suspended GNPs- NH_3 into thermoplastic polyurethane (TPU) in diacetone alcohol, they reported that the suspension could maintain viscosity, shear thinning behavior, and viscoelastic properties over the twelve-week storage time. This was due to the nitrogen species on the GNP surface increased surface polarity and improved wetting between TPU and GNP- NH_3 .

The authors proposed these nitrogen species on CNT- NH_3 or GNP- NH_3 could interact via dipole-dipole interaction with the $\text{C}\equiv\text{N}$ groups in the acrylonitrile segment of the ABS matrix allowing them to be dispersed better than those non-functionalized nanofillers. Since the electrical resistivity of the nanocomposites in this research was measured only at the surface, the influence of the improved dispersion on the measured was not pronounced as observed later in the thermal conductivity measurement. According to Marsden *et al.* [2], doping graphene with heteroatoms such as nitrogen can increase the electrical conductivity of the polymer composites. When increasing the weight ratio of CNT:GNP to be 80:20 wt%, the percolation threshold occurred at the nanofiller concentration of just 2.0 wt%, similarly to incorporating pure CNTs. This confirmed the long aspect ratio of the CNTs helped the percolation network to form at lower loading of carbon-based nanofillers. This finding could be useful for the industrial segment to select the suitable hybrid nanofiller weight ratio and concentration to meet their applications.

3.2 Tensile modulus of ABS/carbon reinforced nanocomposites adding non-functionalized (R1) or ammonia plasma functionalized (NH_3) nanofillers

Since the ABS/carbon reinforced nanocomposites could be used in the IC packaging from ESD charges, mechanical behaviour of these nanocomposites should be investigated in order to understand the impact of carbon-based nanofillers on mechanical properties. The stress-strain curve of neat ABS under a standard tensile strain rate indicates ductile behavior of the ABS matrix due to the presence of yield point and extensive plastic deformation until failure. The neat ABS presents a linear initial slope of elastic deformation and then has a yield point. After reaching the yield point, the stress drops where the plastic deformation occurs which shear-banding and/or crazing is formed inside the specimen and finally the specimen is broken. This mechanical behaviour suggests that the ABS part could withstand the applied stress with good rigidity until reaching the yield point and then it should be the end of its service.

For ABS nanocomposites, the stress-strain curves also present the linear initial slope of elastic deformation with higher stress values of the yield point. The presence of yield point indicates the good dispersion of the nanofillers inside the ABS matrix. After reaching the yield point, the shorter strain at break indicates that the nanocomposite shows the quasi-brittle characteristic, which the crack propagation arises at the interface between the ABS matrix and the nanofillers.

Figure 4 compares tensile modulus of the ABS-based nanocomposites adding non-functionalized (R1) or ammonia plasma functionalized (NH_3) nanofillers. The neat ABS matrix used in this research had the tensile modulus of about 703.80 MPa, which incorporating the carbon-based nanofillers could enhance the rigidity of the ABS matrix depending on the functionalization and the concentration of the nanofillers.

From Figure 4(a), adding only GNP-R1 of 2 wt%, 4 wt%, 6 wt%, and 8 wt% into ABS matrix increased tensile modulus to be 9.61%, 20.57%, 17.02%, and 21.51% higher than that of neat ABS, respectively. In contrast, adding only CNT-R1 of 2 wt%, 4 wt%, 6 wt%, and 8 wt% into ABS matrix further increased tensile modulus to be 14.04%, 17.79%, 33.25%, and 28.42% higher than tensile modulus of neat ABS, respectively. This was attributed to the very much higher fiber aspect ratio of the as-received CNTs than that of the as-received GNPs.

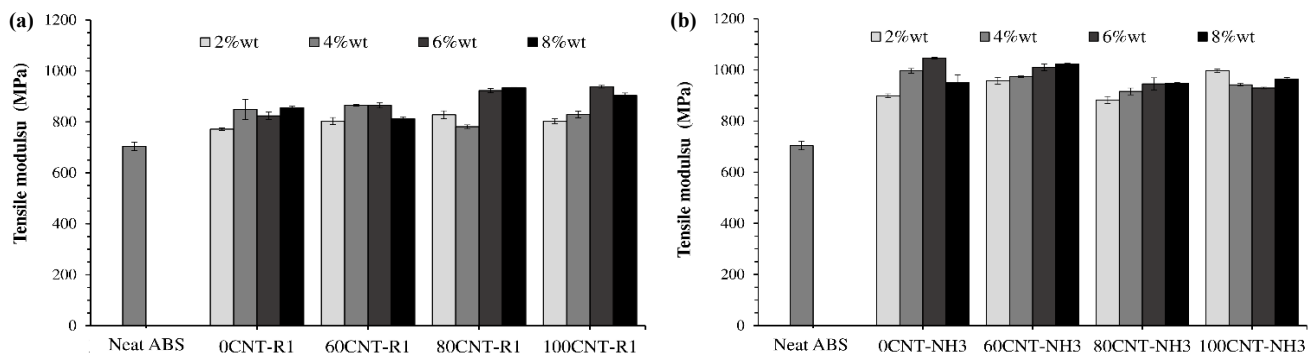


Figure 4. Tensile modulus of neat ABS and ABS/carbon reinforced nano-composites adding (a) non-functionalized or (b) ammonia plasma functionalized hybrid nanofillers.

As discussed previously, the weight ratio of the hybrid CNT-R1: GNP-R1 nanofiller that can reach the percolation threshold for using as a static dissipative material was 60:40. It was found that adding these suitable hybrid nanofillers could enhance the tensile modulus of the nanocomposite to be 14.09%, 22.96%, 22.88%, and 15.37% higher than the modulus of neat ABS, respectively.

When these nanofillers were ammonia plasma functionalization to obtain the nitrogen species on the surfaces, they could be dispersed and distributed in the ABS matrix much better using a twin-screw extruder as evident in the increase percentage of the tensile modulus.

From Figure 4(b), adding only CNT-NH₃ of 2 wt%, 4 wt%, 6 wt%, and 8 wt% into ABS matrix increased the tensile modulus to be 41.54%, 33.82%, 32.07%, and 37.04% higher than the modulus of neat ABS, respectively. According to William *et al.* [16], the ammonia plasma treatment introduced amine, nitrile, amide, and oxime groups onto the surface of the CNTs, which was confirmed by the XPS analysis. They explained that the ammonia surface treatment could add mutual electrostatic repulsion charges to the surface of the CNTs, which gave the CNTs the potential to overcome the binding van der Waals forces and to aid dispersion. The reduction of tensile modulus after the concentration at percolation threshold would be due to the agglomeration of the nanofillers.

In contrast, adding only GNP-NH₃ of 2 wt%, 4 wt%, 6 wt%, and 8 wt% into ABS matrix increased the tensile modulus to be 27.72%, 41.57%, 48.65%, and 34.94% higher than the modulus of neat ABS, respectively. This was due to the good dispersion of the plate-like GNP-NH₃ was achieved during the compounding by the screw elements (i.e. kneading block) of the twin-screw extruder.

Interestingly, the suitable hybrid CNT-NH₃:GNP-NH₃ 60:40 of 2 wt%, 4 wt%, 6 wt%, and 8 wt% could enhance the tensile modulus of ABS to be 35.98%, 38.29%, 43.54%, and 45.48% higher than the modulus of neat ABS, respectively. It should be noted that adding too high loading of these nanofillers [21] could reduce the tensile modulus due to the possible agglomeration of the nanofillers. This was observed in the 0CNT-NH₃ nanocomposite adding the solely GNPs of 8 wt%. This was in agreement with the research of Yang *et al.* [13]. They reinforced epoxy resin with the hybrid mixture of GNPs and MWCNTs, and explained that the increasing mechanical properties of epoxy nanocomposites resulted from stacking of individual two-dimensional GNPs was effectively inhibited by introducing one-dimensional MWCNTs. MWCNTs with long tortuous shape and

could bridge adjacent GNPs and inhibited the aggregation, resulting in a high contact area between the GNP/MWCNT structures and the epoxy matrix.

3.3 Tensile strength of ABS/carbon reinforced nanocomposites adding non-functionalized (R1) or ammonia plasma functionalized (NH₃) nanofillers

Figure 5 compares tensile strength of the ABS-based nanocomposites adding non-functionalized (R1) or ammonia plasma functionalized (NH₃). As shown in the stress-strain curve, the maximum tensile strength of neat ABS and their carbon-based nanocomposites occurred at yield which the plastic deformation took place. The neat ABS matrix had tensile strength at yield of about 40.48 MPa with tensile strain at yield of 6.15%. As seen in Figure 4(a), incorporating pure CNT-R1 of 2 wt%, 4 wt%, 6 wt%, and 8 wt% increased tensile strength of the ABS-based nanocomposites to be 43.54 MPa, 43.98 MPa, 47.88 MPa, and 48.04 MPa, that occurred at strain of 6.28%, 6.16%, 6.42%, and 6.55%, respectively. Since the yielding of the nanocomposites occurred at higher stress and strain, this implied the CNT-R1 was compatible and dispersed well in the ABS matrix.

Meanwhile, incorporating pure GNP-R1 of 2 wt%, 4 wt%, 6 wt%, and 8 wt% of the ABS-based nanocomposites increased tensile strength to be 40.78 MPa, 41.64 MPa, 40.70 MPa, and 41.98 MPa that occurred at strain of 6.07%, 5.98%, 5.98%, and 5.91%, respectively. This implied that the reinforcing effect of CNT-R1 with much higher aspect ratio on ABS matrix was better than that of GNP-R1. Compared to Jagadeesh Chandra *et al.* [22], tensile strength of the ABS reinforced with GNP-R1 or GNP-NH₃ had higher tensile strength due to good physical interaction between the ABS matrix and the GNPs. For a hybrid mixture, tensile strength of the nanocomposites was increased when they were incorporated with higher CNT weight ratio.

From Figure 5(b), tensile strength at yield was increased to be 54.91 MPa, 53.72 MPa, 52.82 MPa, and 52.54 MPa that occurred at strain of 5.15%, 4.99%, 4.84%, and 4.70%, respectively, when adding pure CNT-NH₃ of 2 wt%, 4 wt%, 6 wt%, and 8 wt%. This was attributed to the good dispersion of CNT-NH₃ in the ABS matrix due to the secondary interaction between the acrylonitrile segment and the nitrogen species attached on the CNTs surface. The high aspect ratio of the CNTs reinforced the ABS matrix that the higher tensile stress was required to deform the ABS matrix during the plastic behaviour.

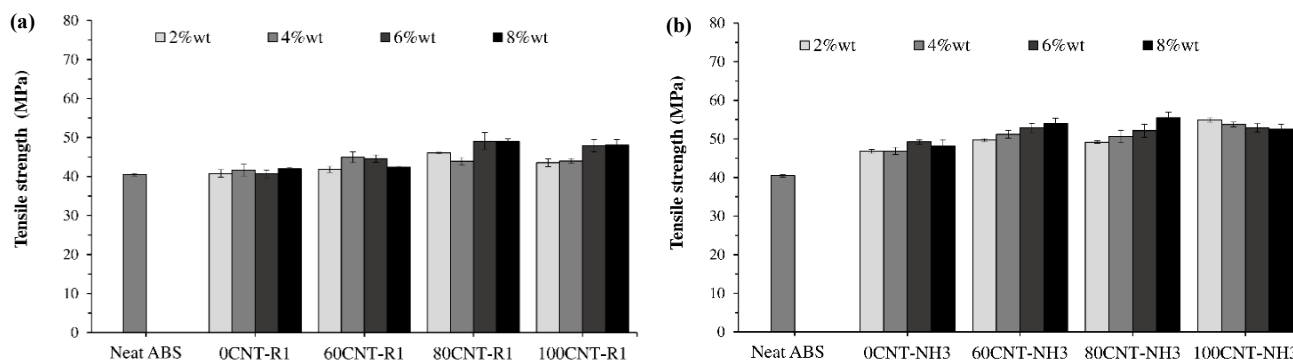


Figure 5. Tensile strength of neat ABS and ABS/carbon reinforced nano-composites adding (a) non-functionalized or (b) ammonia plasma functionalized hybrid nanofillers.

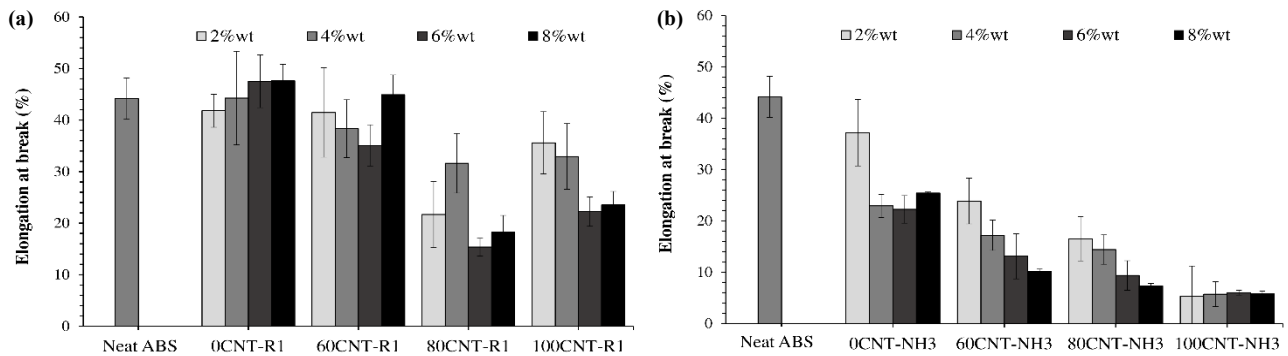


Figure 6. Elongation at break of neat ABS and ABS/carbon reinforced nanocomposites adding (a) non-functionalized or (b) ammonia plasma functionalized hybrid nanofillers.

Tensile strength at yield was increased to be 46.77 MPa, 46.88 MPa, 49.23 MPa, and 48.18 MPa that occurred at strain of 5.24%, 4.98%, 4.83%, and 5.21%, respectively, when adding pure GNP-NH₃ of 2 wt%, 4 wt%, 6 wt%, and 8 wt%. The improvement of functionalization on tensile strength was similar to the work by You *et al.* [15], which tensile strength of polyamide 6,6 (PA66) adding nitrogen-gas plasma treated GNPs increased by more than 110%, compared to those adding non-functionalized nanocomposites. They explained that the improved mechanical properties of the nanocomposites resulted from the uniform dispersion of GNPs in the composites and the improved interfacial affinity between PA66 and GNPs.

3.4 Elongation at break of ABS/carbon reinforced nanocomposites adding non-functionalized (R1) or ammonia plasma functionalized (NH₃) nanofillers

Figure 6 compares elongation at break of the ABS-based nanocomposites adding non-functionalized (R1) or ammonia plasma functionalized (NH₃) nanofillers. The elongation at break of neat ABS was about 44.14%, which incorporating these nanofillers reduced the extension of the ABS matrix unsurprisingly. As shown in Figure 6(a), it is obvious that elongation at break of the ABS/CNT-R1 nanocomposites was reduced significantly than that of the ABS/GNP-R1 nanocomposites with higher nanofiller concentration. This was due to the crack propagation occurred at the interface between the ABS matrix and the CNT-R1 nanofillers. On the other hand, the averages of elongation at break were slightly increased with high standard variations for the ABS nanocomposites adding only GNP-R1. This indicated the specimen failure occurred from the combination between the sheet slippage of GNP nanoplatelets [22,23] and the crack propagation at the specimen necking.

The sheet slippage of GNPs could be supported from the discussion by Weiheng Xu *et al.* [24]. They developed a tri-axial microstructured 3-phase fiber made of polyvinyl alcohol and GNPs (20 wt%) using a dry-jet wet spinning technique, which the alignment of a continuous GNP channel was achieved, resulting in 73.5% and 17.3% improvement in Young's modulus and tensile strength, respectively. They explained that the highly orientation of GNPs could be obtained from the stacked layers in GNPs firstly aligned along the shear-stress direction, followed the slippage of GNP layer with continued shear stress accumulation after complete orientation along the fiber axis.

In contrast, adding the ammonia plasma functionalized nanofillers decreased elongation at break of the nanocomposites in a more pronounced manner as shown in Figure 6(b). Despite of the nanofiller concentration, elongation at break of the ABS/CNT-NH₃ nanocomposites was in the same range of about 5% to 6%. In the other words, tensile failure of these nanocomposites was in brittle manner while the failure of ABS was in the ductile behaviour. Elongation at break of the hybrid nanocomposites was decreased with the higher nanofiller concentration due to the good dispersion of the nanofillers with the NH₃ functionalized nanofillers, which could be confirmed by SEM micrographs.

3.5 Morphology of ABS/carbon reinforced nanocomposites adding non-functionalized (R1) or ammonia plasma functionalized (NH₃) nanofillers

Figure 7 show SEM micrographs of cryo-fractured surface of neat ABS and ABS/CNTs:GNPs nanocomposites, which the micrographs were obtained in the magnification of 1000× for correlation with mechanical performance of the CNT:GNP nanocomposites. It is seen that neat ABS surface in Figure 7(a) is virtually smooth with distributed shallow ripples implying ductile fracture behaviour from rubbery phase of butadiene segment although the specimen was broken at the cryo-state. In Figure 7(b), the fracture surface of the 0CNT-R1(4) nanocomposite presents rough surface consisted of plains and valleys that were distributed all over the fracture surface. This indicates the presence of the GNP-R1 of 4 wt% that were distributed inside the ABS matrix. The cryo-fractured specimen presents ductile behaviour of the ABS matrix, however, the fracture occurred mainly at the interface between the ABS matrix and the distributed GNP-R1.

The fracture surface of the 0CNT-NH₃(4) nanocomposite in Figure 7(c) presents rougher surface consisted of hills and deep valleys that were distributed all over the fracture surface. This implied the GNP-NH₃ was distributed better inside the ABS matrix. These finding correlated with the reduction of elongation at break significantly when incorporating these GNP-NH₃ into the ductile ABS matrix. It should be noted that the visible bright spots on the surface are GNP aggregates that are protruded from the fracture surface. According to Weikang Li *et al.* [23], they reinforced epoxy resin with either CNTs or GNPs and observed that GNPs were aggregated in the epoxy matrix and CNTs were much easier to be dispersed than GNPs. They discussed

that the van der Waals forces resulted from the plane-to-plane contact of the adjacent GNPs may be stronger than that of CNTs. The bright spots from the GNP aggregates are also reported by Benlikaya *et al.* [25].

Figure 7(d-e) show the fracture surface of the 60CNT-R1(4) and 60CNT-NH₃(4) nanocomposites, respectively. They also present rough surface consisted of hills and deep valleys that were distributed all over the fracture surface. However, the 60CNT-NH₃(4) nanocomposite present relatively ductile-to-brittle behaviour as seen by the continued edge that indicates the crack propagation direction. The visible bright spots due to GNP aggregates are also observed.

Figure 7(f-g) show the fracture surface of the 0CNT-R1(4) and 100CNT-NH₃(4) nanocomposite, respectively. Compared to the others, these SEM micrographs clearly indicate brittle behaviour of the cryo-fractured failure. The fractured surface presents rough surface consisted of plains and valleys resemble the terraces, especially for the nano-composite adding CNT-NH₃. The fractured surface of the 100CNT-NH₃(4) presents the traces of embedded CNTs with better dispersion of the nanofillers. This implies good interfacial adhesion between the ABS matrix and the ammonia plasma functionalized nanofiller.

3.6 Thermal conductivity of ABS/carbon reinforced nanocomposites adding non-functionalized (R1) or ammonia plasma functionalized (NH₃) nanofillers

When electronic/electrical devices are in service, the heat could be generated inside the housing due to the conversion of electrical energy into electric heating, which could cause overheating or rising temperatures in an electrical circuit that possibly damages the electrical circuit itself. Heat transfer of the electronic/ electrical devices could be designed via heat conduction or heat convection. Since these nanofillers are graphite-like, the heat can be dissipated thoroughly in the polymer matrix. Thus, it would be useful to investigate thermal conductivity of these nanocomposites.

Figure 8 and Figure 9 show thermal conductivity of the ABS nanocomposites reinforced with CNTs, GNPs, and their hybrid mixture

in various concentrations. Neat ABS had thermal conductivity value of 2.08×10^{-1} W/mK, which the values were increased when adding these carbon-based nanofillers. Comparison between CNTs and GNPs, it was found that adding pure GNPs in the same concentration improved thermal conductivity of thermal-insulating ABS matrix better than adding only pure CNTs. Moreover, too high concentration of CNTs (8 wt%) incorporated into the ABS matrix resulted the lowest thermal conductivity. These was attributed to the higher surface area of the graphene nanoplatelets that these graphene panes could form the thermal conductive network.

The similar phenomena was reported by Caradonna *et al.* [12], which they presented experimental results that thermal conductivity of the epoxy/GNP composites increased in a linear fashion with the increase of GNP concentration (0.5 wt% to 30 wt%). In contrast, the capability for thermal conductivity enhancement by CNTs, which is expected to have great impact, is greatly limited by their tremendous surface area, and then by the strong phonon boundary scattering occurring at the interface with the polymer matrix.

Comparison among the nanofillers, it was clearly seen that the NH₃-plasma functionalized nanofillers enhanced thermal conductivity of the ABS matrix much better than the non-functionalized ones. The maximum thermal conductivity was reached when adding only the CNT-NH₃ of 6 wt%. This implied that the nitrogen species on the ammonia plasma functionalized nanofillers could interact via dipole-dipole interaction with the C≡N groups in the acrylonitrile segment of the ABS matrix.

Possibly, the electron from the π - π conjugated structure of CNTs may interact with the π - π conjugated structure in any styrene segment. This kind of interaction was described in the report by Delgado-Gonzalez *et al.* [26] that the possibility of an intermolecular interaction between the Cyanine dye and the aminomethyl cross-linked polystyrene nanoparticles. The close proximity of the Cyanine dye aromatic rings and conjugated system (alternating double bonds) to the polystyrene aromatic groups was considered to promote the π - π stacking interactions, causing a charge transfer that resulted in the green emissive transition.

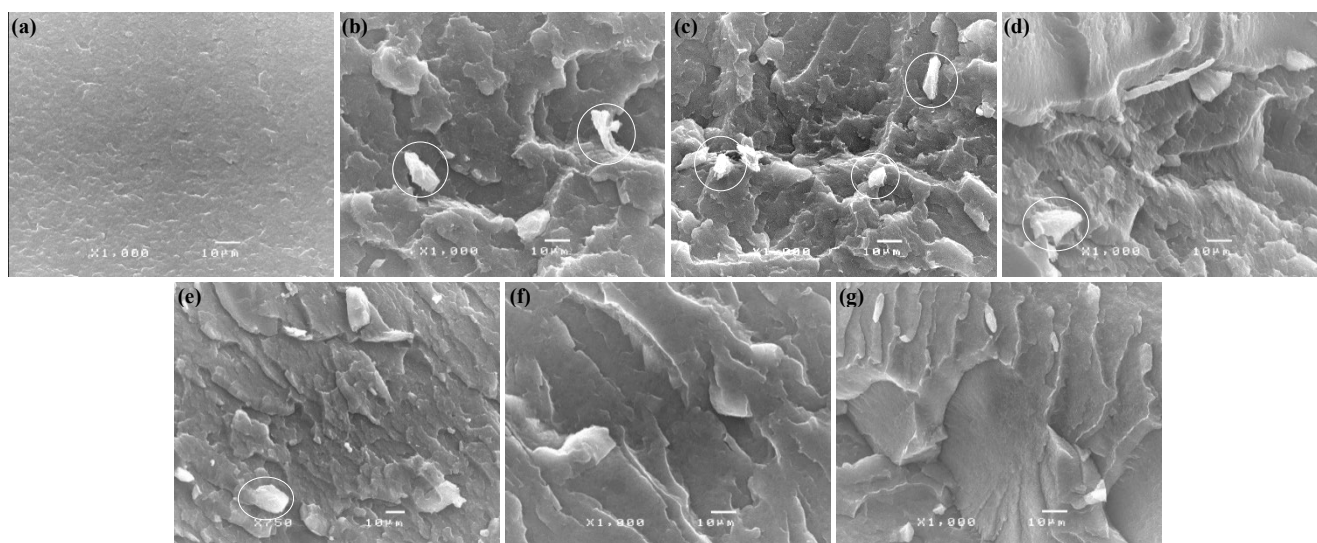


Figure 7. SEM micrographs (magnification of 1000 \times) of cryo-fractured surface of (a) neat ABS, (b) 0CNT-R1(4), (c) 0CNT-NH₃(4), (d) 60CNT-R1(4), (e) 60CNT-NH₃(4), (f) 100CNT-R1(4), and (g) 100CNT-NH₃(4) nanocomposites.

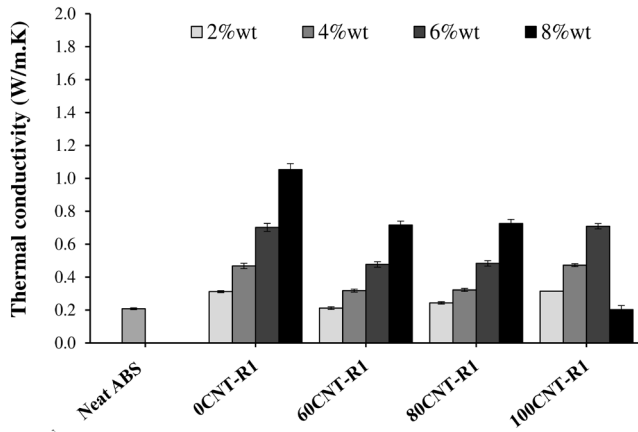


Figure 8. Thermal conductivity of neat ABS and ABS/non-functionalized (R1) carbon-based nanocomposite.

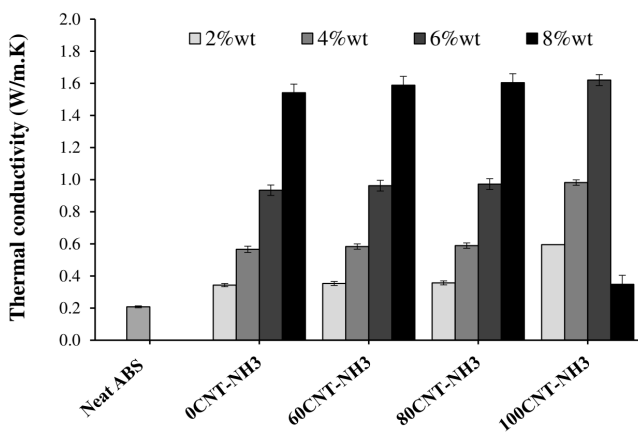


Figure 9. Thermal conductivity of neat ABS and ABS/ammonia plasma functionalized (NH₃) carbon-based nanocomposite.

Benlikaya *et al.* [25] prepared ammonia plasma CNTs and then compounded with epoxy resin, which they studied the interaction between the active species on CNT-NH₃ and the epoxy resin. They found the IR chemical shift of the wavelengths in Diglycidyl ether of bisphenol A (DGEBA) and hexahydro-4-methylphthalic anhydride (HMPA) that indicated their interactions with CNT-NH₃. After the curing reaction, the overlapping of IR peaks confirmed the reactions between the fillers and the components and the ones between all components.

4. Conclusions

The influence of functionalization and concentration of a hybrid carbon-based nanofillers (CNTs:GNPs) on electrical, mechanical, and thermal properties of ABS was investigated by preparing masterbatch and then diluting with the neat polymer to the desired concentrations of 2 wt%, 4 wt%, 6 wt%, and 8 wt%. It was found that functionalization these nanofillers with ammonia gas via plasma treatment to obtain nitrogen species increased better dispersion of nanofillers in the ABS matrix. When using a hybrid nanofillers in the weight ratio of 60:40 wt%, it was found that the percolation threshold could be reached with a concentration of 4 wt%, which the surface electrical resistivity of the NH₃-hybrid nanocomposites was reduced more than

those adding the R1-hybrid nanofillers. At this suitable weight ratio, tensile modulus and tensile strength of the CNT-NH₃:GNP-NH₃ 60:40 of 2 wt%, 4 wt%, 6 wt%, and 8 wt% could enhance the tensile modulus the best. Moreover, the NH₃-plasma functionalized nanofillers enhanced thermal conductivity of the ABS matrix much better than the non-functionalized ones.

Acknowledgements

The authors would like to thank the IRPC Public Co., Ltd and Haydale Technologies Co. Ltd. for their materials support. The Department of Materials Science and Engineering, Faculty of Engineering and Industrial Technology, Silpakorn University, is appreciated for the author's assistant teaching scholarship. In addition, the Faculty of Engineering and Technology King Mongkut's University of Technology North Bangkok, Rayong campus, is appreciated for research facilities during the Covid pandemic situation.

References

- [1] Omnesus. "Comprehensive guide on Acrylonitrile Butadiene Styrene (ABS)." <https://omnexus.specialchem.com/selection-guide/acrylonitrile-butadiene-styrene-abs-plastic> (accessed March 18, 2024).
- [2] A. J. Marsden, D. G. Papageorgiou, C. Vallés, A. Liscio, V. Palermo, M. A. Bissett, R. J. Young, and I. A. Kinloch, "Electrical percolation in graphene-polymer composites," *2D Materials*, vol. 5, pp. 032003, 2018.
- [3] N. Saravanan, R. Rajasekar, S. Mahalakshmi, T. Sathishkumar, K. Sasikumar, and S. Sahoo, "Graphene and modified graphene-based polymer nanocomposites – A review," *Journal of Reinforced Plastics and Composites*, vol. 33, no. 12, pp. 1158-1170, 2014.
- [4] VersaLogic, "The Invisible Foe – Understanding and Controlling ESD Damage," *A VersaLogic Focus on Reliability White Paper*.
- [5] T. F. d. Silva, F. Menezes, L. S. Montagna, A. P. Lemes, and F. R. Passador, "Preparation and characterization of antistatic packaging for electronic components based on poly(lactic acid)/carbon black composites," *Journal of Applied Polymer Science*, vol. 136, no. 1, pp. 47273, 2018.
- [6] S. Zhang, X. Xu, T. Lin, and P. He, "Recent advances in nanomaterials for packaging of electronic devices," *Journal of Materials Science: Materials in Electronics*, vol. 30, pp. 13855-13868, 2019.
- [7] W. Sriseubsai, A. Tippayakraisorn, and J. W. Lim, "Robust design of PC/ABS filled with nano carbon black for electromagnetic shielding effectiveness and surface resistivity," *Processes*, vol. 8, no. 5, p. 616, 2020.
- [8] M. H. Al-Saleh, "Clay/carbon nanotube hybrid mixture to reduce the electrical percolation threshold of polymer nanocomposites," *Composites Science and Technology*, vol. 149, pp. 34-40, 2017.
- [9] S. Duangsripat, and C. Polprasert, "Production and cost benefit analysis of biodegradable poly(lactic acid)-epoxidized palm oil blend/graphene nanocomposite," in *The 4th International Symposium on Engineering, Energy and Environment*, Thammasat

- University, Pattaya Campus, Thailand, P. Wangskarn, Ed., 8-10 November 2015: Thammasat University, Nagaoka University of Technology, Saitama University and Tokyo Institute of Technology (Tokyo Tech),
- [10] M. Mokhtari, E. Archer, N. Bloomfield, E. Harkin-Jones, and A. McIlhagger, "High-performance and cost-effective melt blended poly(etheretherketone)/expanded graphite composites for mass production of antistatic materials," *Polymer International*, vol. 70, pp. 1137–1145, 2021.
- [11] X. Lu, Y. Liu, L. Pichon, D. He, O. Dubrunfaut, and J. Bai, "Effective electrical conductivity of CNT/polymernanocomposites," in *International Symposium on Electromagnetic Compatibility-EMC EUROPE*, Rome, France, 2020, pp. 1-4.
- [12] C. B. A. Caradonna, E. Padovano, and M. Pietroluongo, "Electrical and thermal conductivity of epoxy-carbon filler composites processed by calendaring," *Materials (Basel)*, vol. 12, no. 9, pp. 1522, 2019.
- [13] S. Yang, W. Lin, Y. Huang, H. Tien, J. Wang, C. Ma, S. Li, and Y. Wang, "Synergetic effects of graphene platelets and carbon nanotubes on the mechanical and thermal properties of epoxy composites," *Carbon*, vol. 49, no. 3, pp. 793-803, 2011.
- [14] Z. Yan, X. Zhang, Y. Gao, Z. Kong, X. Ma, Q. Gou, H. Liang, X. Cai, H. Tan, and J. Cai, "Anisotropy induced in magnetic field in GNPs/epoxy composites used as an effective heat dissipation electronic packaging material," *Journal of Applied Polymer Science*, vol. 140, no. 42, 2023.
- [15] J. You, H.-H. Choi, J. Cho, J. G. Son, M. Park, S.-S. Lee, and J. H. Park, "Highly thermally conductive and mechanically robust polyamide/graphite nanoplatelet composites via mechanochemical bonding techniques with plasma treatment," *Composites Science and Technology*, vol. 160, pp. 245-254, 2018.
- [16] J. Williams, W. Broughton, T. Koukoulas, and S. S. Rahatekar, "Plasma treatment as a method for functionalising and improving dispersion of carbon nanotubes in epoxy resins," *Journal of Materials Science*, vol. 48, pp. 1005-1013, 2013.
- [17] Haydale. "HDPlas™ GNPs Plasma functionalised graphene nanoplatelets." <https://www.graphene-info.com/files/graphene/HDPlas-GNP-Technical-Sheet-2.03.pdf> (accessed August 8, 2023).
- [18] S. Dul, A. Pegoretti, and L. Fambri, "Effects of the nanofillers on physical properties of Acrylonitrile-Butadiene-Styrene nanocomposites: comparison of graphene nanoplatelets and multiwall carbon nanotubes," *Nanomaterials*, vol. 8, pp. 674, 2018.
- [19] J. Du, L. Zhao, Y. Zeng, L. Zhang, F. Li, P. Liu, and C. Liu, "Comparison of electrical properties between multi-walled carbon nanotube and graphene nanosheet/high density polyethylene composites with a segregated network structure," *Carbon*, vol. 49, no. 4, pp. 1094-1100, 2011.
- [20] A. Claypole, J. Claypole, T. Claypole, D. Gethin, and L. Kilduff, "The effect of plasma functionalization on the print performance and time stability of graphite nanoplatelet electrically conducting inks," *Journal of Coatings Technology and Research*, vol. 18, no. 1, pp. 193-203, 2021.
- [21] M. Alberto, M. Iliut, M. K. Pitchan, J. Behnsen, and A. Vijayaraghavan, "High-grip and hard-wearing graphene reinforced polyurethane coatings," *Composites Part B: Engineering*, vol. 213, pp. 108727, 2021.
- [22] R. B. J. Chandra, B. Shivamurthy, M. S. Kumar, N. N. Prabhu, and D. Sharma, "Mechanical and electrical properties and electromagnetic-wave-shielding effectiveness of graphene-nanoplatelet-reinforced Acrylonitrile Butadiene Styrene nanocomposites," *Journal of Composite Science*, vol. 7, pp. 117, 2023.
- [23] W. Li, A. Dichiaro, and J. Bai, "Carbon nanotube-graphene nanoplatelet hybrids as high-performance multifunctional reinforcements in epoxy composites," *Composites Science and Technology*, vol. 74, pp. 221-227, 2013.
- [24] W. Xu, S. Jambhulkar, R. Verma, R. Franklin, D. Ravichandran, and K. Song, "In situ alignment of graphene nanoplatelets in poly(vinylalcohol) nanocomposite fibers with controlled stepwise interfacial exfoliation," *Nanoscale Advances*, vol. 1, pp. 2510-2517, 2019.
- [25] R. Benlikaya, P. Slobodian, P. Riha, H. Puliyalil, U. Cvelbar, and R. Olejnik, "Ammonia plasma-treated carbon nanotube/epoxy composites and their use in sensing applications," *Express Polymer Letters*, vol. 16, no. 1, pp. 85-101, 2022.
- [26] A. Delgado-Gonzalez, E. Garcia-Fernandez, T. Valero, M. V. Cano-Cortes, M. J. Ruedas-Rama, A. Unciti-Broceta, R. M. Sanchez-Martin, J. J. Diaz-Mochon, and A. Orte, "Metallo-fluorescent nanoparticles for multimodal applications," *ACS Omega*, vol. 3, no. 1, pp. 144-153, 2018.